

# Melting of phase change materials (NPCMs) in trapezoidal cavity

Farida IACHACHENE, Zoubida HADDAD

**Abstract**—The present study aims to analyze solidification of nanoparticles-enhanced phase-change materials (NPCM) in trapezoidal cavity at two different orientations, using enthalpy–porosity method. The horizontal walls of the cavities are insulated while side walls are maintained at constant temperatures. The paraffin wax is used as the phase change material (PCM) and graphene as the nanomaterial. The study is governed by tracing the melting front at various times for PCM and NPCM. In addition, the evolution of streamlines and isotherms is presented at different temperature differences. It was observed that adding nanoparticles does not enhance the melting. However, higher melting is attained by changing the orientation of the cavity.

**Index Terms**— Trapezoidal cavity, melting Phase change materials (PCM), Nanofluid, Computational fluid dynamics (CFD).



## 1 INTRODUCTION

A continuous increase in the gap between the energy demand and supply and the depletion of fossil fuels have received the attention of researchers in the last few decades. This increasing demand forces researchers to develop renewable energy sources. One of the main concerns in thermal energy management is to practice materials having high energy storage capacity with high reliability and less aging effect. In the recent past, there has been huge amount of research efforts devoted to developing such novel materials for variety of applications, such as buildings, textiles, and space heating. These materials are commonly known as PCM, are promising thermal storage materials for storing and discharging bulk amounts of latent heat throughout with regulated time intervals associated as per energy demand. Though, the criteria for the choice of PCM for a specific application is its melting temperature, but other properties such as the latent heat of fusion,

thermal conductivity, thermal stability, density and lower volume change, also play significant role in better designing of a product and therefore these are essential to be considered. However, low thermal conductivity is the major drawback of latent thermal energy storage of PCMs, which decreases the melting/solidification rate, and seriously limits their practical applications.

In order to enhance heat transfer in PCM, several techniques have been proposed such as using microencapsulated PCM [1],

multiple PCM [2], finned tubes with different configurations [3], heat pipes [4] and dispersing highly conductive particles in

PCM. The subject of this study is the last approach where solid particles distributed in PCM are in nano size.

The first reported work on the improvement introduced by nanoparticle-enhanced phase change materials (NEPCM) was performed by Khodadadi and Hosseinzadeh[5]. They reported that the latent heat of PCM would decline and the discharge time decreased when the mass fraction of dispersed particles was increased. The effect of dispersion of Cu nanoparticles on the melting performance of n-paraffin inside an annular cavity between two concentric cylinders was presented by Sebt et al. [6]. They illustrated that suspension of nano-Cu particles augmented the thermal conductivity and heat transfer and consequently

- Farida IACHACHENE, Department of physic, faculty of sciences, University M'Hamed Bougara Boumerdes, Algeria iachachenef@yahoo.fr
- Zoubida HADDAD Institute of Electrical and Electronic Engineering (IGEE), University M'Hamed Bougara Boumerdes, Algeria h\_zoubida@hotmail.com

shortened the melting time. On the other hand, the volume of storage material will be decreased as the nanoparticle concentration increased. Feng et al. [7] investigated numerically the melting of water–Cu nanoparticles in a bottom-heated rectangular cavity and concluded that the NPCM exhibits high heat transfer efficiency in comparison to the pure PCM. They also showed that as the volume fraction of nanoparticles increases, the temperature field and melting interface evolves faster, and the melt fraction and energy stored increases. A numerical study on the heat transfer during process of conduction dominated solidification of copper–water nanofluid in isosceles trapezoidal cavity was presented by Sharma et al. [8]. The results revealed that the heat transfer performance of NPCM is significantly enhanced with the use of a trapezoidal cavity when compared to a square cavity having the same internal area. Recently, Arici et al. [9] undertook a numerical study on the melting of paraffin wax with  $\text{Al}_2\text{O}_3$  nanoparticles in a partially heated and cooled square cavity. They illustrated that the heat energy stored by PCM can be enhanced by changing orientation of thermally active walls of the enclosure, dispersing nanoparticules or applying both simultaneously.

TABLE 1  
THERMO-PHYSICAL PROPERTIES OF PCM AND GRAPHENE CONTAINER [9, 10].

Property	Paraffin wax	Graphene
Melting point (°C)	46	-
Latent heat of fusion (kJ/kg)	173,400	-
Density (kg/m <sup>3</sup> )	$\frac{750}{0.001(T - 319.15) + 1}$	2200
Specific heat (kJ/kg K)	2.89	0.7901
Thermal conductivity (W/m_K)	0.21 if $T < T_{\text{solidus}}$ 0.12 if $T > T_{\text{liquidus}}$	5000
Viscosity (Ns/m <sup>2</sup> )	$0.001 \exp\left(-4.25 + \frac{1790}{T}\right)$	-

The purpose of the present work is to analyse the melting of the paraffin wax with Graphene nanoparticles filled in a trapezoidal cavity using the Ansys-Fluent CFD commercial package. The effects of temperature difference, and the orientation of the cavity at two different positions on the melting process will be presented.

## 2 METHODOLOGY

### 2.1 Geometry and boundary conditions

A schematic view of the physical model is shown in Fig. 1. The system is made of a trapezoidal cavity with equal length and height ( $L=H=1\text{cm}$ ). The cold wall is maintained at  $T_c = 317.5\text{ K}$  and the hot wall is kept at constant temperature  $T_h$  higher than the melting temperature, while the other sides are maintained adiabatic. Two orientations of the trapezoidal cavity of the same area are considered: in case (I), the cavity has the larger base of length  $L$ , and in case (II), the cavity has the smaller base of length  $L'$ . The cavity is filled with paraffin wax containing graphene nanoparticles, which is assumed to be initially at a temperature slightly below the fusion point.

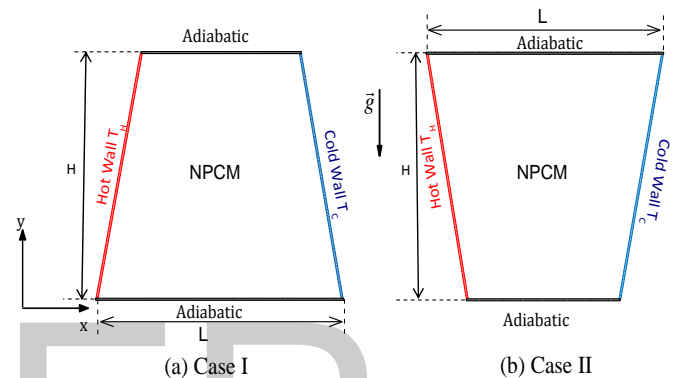


Fig. 1. Computational model and dimensions.

### 2.2 Mathematical formulations

The melting of nanoparticle enhanced PCM is assumed to be Newtonian and incompressible. The flow caused due to the melting is laminar and the viscous dissipations, thermal radiation, and three-dimensional convection are negligible. Thermophysical properties of PCM are temperature dependent, and the melting of PCM is conduction and convection controlled. The graphene nanoparticles are homogeneously distributed in the PCM. The thermo-physical properties of PCM and graphene are represented in Table 1.

Considering the nanofluid as a continuous media with thermal equilibrium between the base fluid and the solid nanoparticles, the governing equations for conservation of mass, momentum and energy can be expressed as:

$$\frac{\partial \rho_{npcm}}{\partial t} + \frac{\partial (\rho_{npcm} U)}{\partial t} + \frac{\partial (\rho_{npcm} V)}{\partial t} = 0 \quad (1)$$

$$\frac{\partial (\rho_{npcm} U)}{\partial t} + \frac{\partial (\rho_{npcm} UU)}{\partial x} + \frac{\partial (\rho_{npcm} UV)}{\partial y} = -\frac{\partial P}{\partial x} + \frac{\partial}{\partial x} \left( \mu_{npcm} \frac{\partial U}{\partial x} \right) + \frac{\partial}{\partial y} \left( \mu_{npcm} \frac{\partial U}{\partial y} \right) + S_x \quad (2)$$

$$\frac{\partial (\rho_{npcm} V)}{\partial t} + \frac{\partial (\rho_{npcm} UV)}{\partial x} + \frac{\partial (\rho_{npcm} VV)}{\partial y} = \frac{\partial P}{\partial y} + \frac{\partial}{\partial x} \left( \mu_{npcm} \frac{\partial V}{\partial x} \right) + \frac{\partial}{\partial y} \left( \mu_{npcm} \frac{\partial V}{\partial y} \right) + (\rho\beta)_{npcm} g (T - T_m) + S_y \quad (3)$$

$$\frac{\partial (\rho_{npcm} H)}{\partial t} + \frac{\partial (\rho_{npcm} UH)}{\partial x} + \frac{\partial (\rho_{npcm} VH)}{\partial y} = \frac{\partial}{\partial x} \left( k_{npcm} \frac{\partial T}{\partial x} \right) + \frac{\partial}{\partial y} \left( k_{npcm} \frac{\partial T}{\partial y} \right) \quad (4)$$

In the above equations, S represents source term which is defined as [12]:

$$S_x = \frac{(1-f)^2}{f^3 + \varepsilon} A_{mush} U, S_y = \frac{(1-f)^2}{f^3 + \varepsilon} A_{mush} V \quad (5)$$

where  $\varepsilon=0.001$  to prevent division by zero,  $A_{mush}$  is the mushy zone constant ( $10^7$  kg/m<sup>3</sup>s) and  $f$  is the liquid volume fraction.

The enthalpy formulation requires a single domain in which the same set of governing equations are used to model both solid and liquid phases of a PCM [11]. The transition from solid to liquid, and vice versa, occurs over a finite temperature range ( $\Delta T$ ) generating an artificial mushy region at the solid-liquid interface. The fluid velocity within the mushy region varies from zero (at the solid boundary) to the natural convection velocity (at the liquid boundary) as the melt fraction varies from 0 to 1. In both cases, phase change is quantified through the following equation for the melt fraction:

$$f = \begin{cases} 0 & \text{if } T < T_{solidus} \\ \frac{T - T_{solidus}}{T_{liquidus} - T_s} & \text{if } T_{solidus} \leq T \leq T_{liquidus} \\ 1 & \text{if } T > T_{liquidus} \end{cases} \quad (6)$$

Different parameters are used in Eqs. (1)–(4) to represent thermophysical properties of liquid and solid forms of nano-PCM. Detailed descriptions and expressions of these parameters are presented in this section.

Density of the nano-PCM can be expressed according to [12] as follows

$$\rho_{npcm} = \phi \rho_{np} + (1 - \phi) \rho_{pcm} \quad (7)$$

where  $\phi$  is the volume fraction of the nanoparticles,  $\rho_{pcm}$  is the density of the base-PCM, and  $\rho_{np}$  is the density of the nanoparticles.

The heat capacitance ( $q_{cp}$ ) of the nano-PCM [12] is given by

$$(\rho C_p)_{npcm} = \phi (\rho C_p)_{np} + (1 - \phi) (\rho C_p)_{pcm} \quad (8)$$

Brinkman model [13] is used to obtain the viscosity of the nano-PCM containing a diluted suspension of small spherical particles and can be expressed as

$$\mu_{npcm} = \frac{\mu_{pcm}}{(1 - \phi)^{2.5}} \quad (9)$$

The thermal conductivity of the nano-PCM can be determined from Maxwell–Garnett (MG) model [14] and is given below

$$k_{npcm} = \frac{k_{np} + 2k_{pcm} - 2\phi(k_{pcm} - k_{np})}{k_{np} + 2k_{pcm} + \phi(k_{pcm} - k_{np})} k_{pcm} \quad (10)$$

where  $k_{pcm}$  is the thermal conductivity of the PCM, and  $k_{np}$  is the thermal conductivity of the nanoparticles.

Thermal conductivity of the NPCM depending on the phase change is expressed as:

$$k_{pcm} = \begin{cases} k_s & \text{if } T < T_{solidus} \\ (1 - f)k_s + f k_l & \text{if } T_{solidus} \leq T \leq T_{liquidus} \\ k_l & \text{if } T > T_{liquidus} \end{cases} \quad (11)$$

where  $k_s$  and  $k_l$  are the thermal conductivity of PCM in solid and liquid phases, respectively.

The latent heat of a nanofluid is determined by [15]

$$(\rho L)_{npcm} = (1 - \phi) (\rho L)_{pcm} \quad (12)$$

### 2.3 Numerical solution setup

The numerical solution is obtained by using the commercial software Ansys Fluent 16.0 which is based on the finite volume method. The simulations were performed using the pressure-based model, which is suitable for the melting and solidification model in ANSYS. A second-order upwind discretization scheme was used to solve the momentum and energy equations; the PRESTO scheme was selected for the pressure correction equation; and the semi-implicit method for pressure-linked equations (SIMPLE) algorithm was used for the pressure–velocity coupling. The under-relaxation factors for the pressure correction, velocity components, thermal energy, and liquid fraction are 0.3, 0.7, 0.95, and 0.9, respectively. The convergence criteria are set at  $10^{-6}$  for the continuity and momentum equations and at  $10^{-10}$  for the energy equation. The time step is 0.1 s, with a maximum of 100 iterations being performed along the entire domain for each timestep. A User Defined Function (UDF) is written to incorporate temperature and phase dependent thermophysical properties of NPCM into ANSYS Fluent.

The computational model is validated against the experimental results of Gau and Viskanta [16] and the numerical predictions of Brent et al. [17] for a melting of Gallium in a rectangular enclosure at  $Pr = 0.0216$ ,  $Ste = 0.039$ , and  $Ra = 6 \times 10^5$ . Fig. 2 shows the melt front of Gallium at several times during the melting process. It can be seen that

the present model predicts well the experimental data and is adequate for solid-liquid phase change problems with convection. The small discrepancy between the predicted melting interface of the developed model and the experimental results may be explained by three possible reasons. First, it is difficult to ensure the heat and cold walls at a desired temperature in the experiment. Second, we did not take into account the temperature dependence in the physical properties of Gallium, and third, the three-dimensional effects are neglected

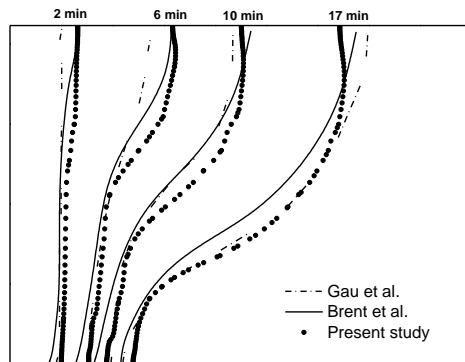


Fig.2. Comparison of melting front at various times obtained by the present study and previously reported works

### 3 RESULTS AND DISCUSSION

#### 3.1 Effect of $\Delta T$ on the melting of pure PCM:

The melting front at various times considering the orientation effect is presented in Fig.3 at  $\Delta T=20^\circ\text{C}$  and  $\Delta T=50^\circ\text{C}$ . As expected, the solid-liquid interface, being an isotherm itself, always intersects the adiabatic top and bottom boundaries. Both cases exhibit the same qualitative melting characteristics. At the initial period of melting process, the melting front moves parallel to the heated wall. After a certain time, the interface exhibits a curvature in the upper portion and remains vertical in the lower region. From this point in time, the entire interface is curved and moves faster in the upper than in the lower portion. This is, of course, due to the fact that the temperature of the paraffin decreases as it flows down the solid-liquid interface, and the temperature gradients (and so the melting rates) is larger in the upper than in the lower portion of the enclosure. In addition, as it can be seen, the effect of increased Rayleigh number (i.e., temperature difference) on the melting is to enhance the melting, and hence, increase the intensity of the natural convection in the melt cavity.

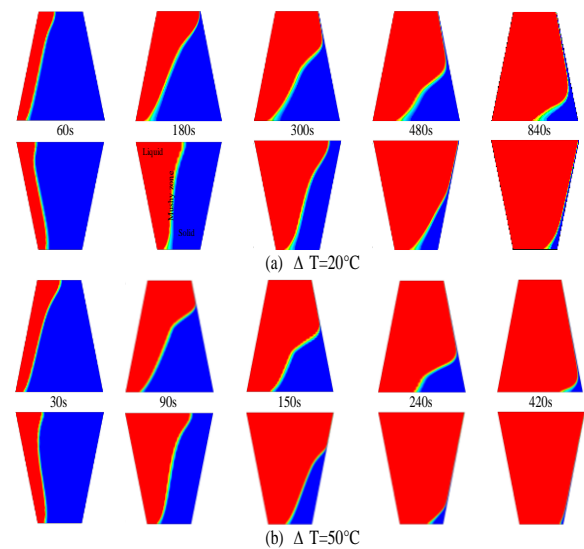


Fig.3. Melting front at different times a)  $\Delta T=20^\circ\text{C}$ , and b)  $\Delta T=50^\circ\text{C}$ .

Fig.4 depicts the time evolution of the streamlines and isotherms for both orientations of the cavity for pure PCM at times of 30s, 60 s, 120, 180 s, 250 s, 480s, and 840 s at  $\Delta T=20^\circ\text{C}$ . For case I (see Fig.4a), as it can be observed, the melting process is divided into three successive regimes. At  $t < 60$  s, heat transfer in the melt region is conduction predominated, and the isotherms are parallel to the heated wall. A unicellular flow which rotates in clockwise direction is established near the heated wall. As time elapses to  $t=120$  s, convection develops in the upper portion of the melting zone, and the size of the cell increases as melting proceeds. However, conduction still prevails in the lower portion. At  $t > 250$  s, a convection dominated regime establishes in the cavity, and the cell reaches to the right wall. For case II (see Fig.4b), it can be seen that the melting process is the same, and the displayed isotherms and streamlines are unchanged. However, the convective regime advances faster.

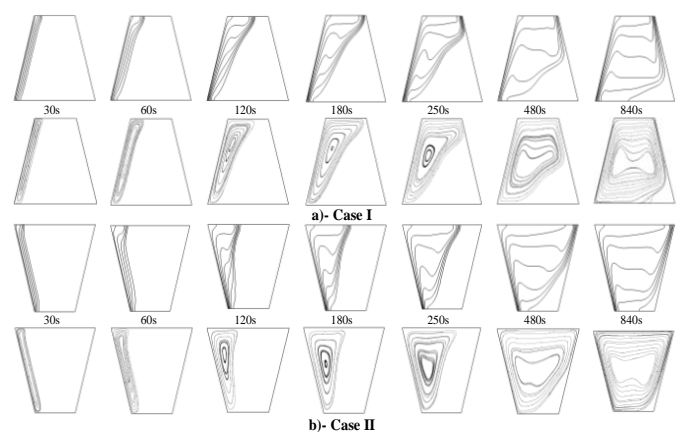


Figure 4 Isotherms and streamlines at different times a) case I, and b) case II.

To better understand the melting process, the instantaneous liquid fraction of pure PCM is shown in Fig.5 for both orientation of the trapezoidal cavity at different temperature differences up to  $\Delta T=50^\circ\text{C}$ . As seen in the figure, at  $t < t_c$ , the liquid fraction curves for both cases overlap since conduction is the principle mode of heat transfer. After this time, the melting rate is enhanced due to the onset of convection in the cavity. As expected, the melting rate increases more rapidly for higher Rayleigh numbers. One may notice that the orientation of the cavity significantly affects the melting rate. It appears that during a convective dominated regime, and at a certain time, the melting rate for case II at  $\Delta T=20^\circ\text{C}$ ,  $\Delta T=30^\circ\text{C}$ ,  $\Delta T=40^\circ\text{C}$  is almost similar to the melting rate of case I at  $\Delta T=30^\circ\text{C}$ ,  $\Delta T=40^\circ\text{C}$ , and  $\Delta T=50^\circ\text{C}$ , respectively. This result indicates that that more energy can be stored for case II than case I for the same temperature difference.

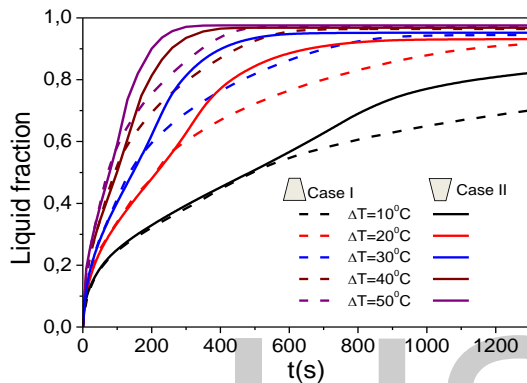


Fig.5. Variations of melt front with time and different temperature difference.

The variation of melting front at  $\Delta T=20^\circ\text{C}$  is reproduced in Fig.6. as it can be seen the melting process may be divided into three phases:

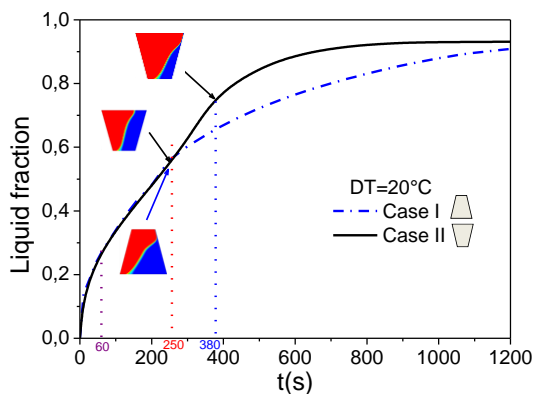


Fig.6. melt front variation at  $\Delta T=20^\circ\text{C}$  with time for both cases.

**Phase I:**  $t < 60\text{s}$ , the melting is achieved by conduction. The liquid fraction rate is consistent for the two orientations.

**Phase II:** for case I:  $60\text{s} < t < 250\text{s}$  and case II:  $60\text{s} < t < 380\text{s}$ .

For the case I, the melting process is accelerated to  $t = 250\text{s}$ , where all the PCM adjacent to the upper wall is melted. The heat transfer due to natural convection becomes the prevailing mode of heat transfer, which can also be inferred from the distorted isotherm lines. However, this phase is longer in case 2, it is prolonged until  $t = 380\text{s}$  where all the PCM in contact with the upper wall is melted.

**Phase III:** for case I:  $t > 250\text{s}$  and case II:  $t > 380\text{s}$ . In this stage the melting rate significantly slows down after the two initial stages and keeps at a slow rate until the PCM is totally melted.

### 3.2 Effect of nanoparticle on melting time:

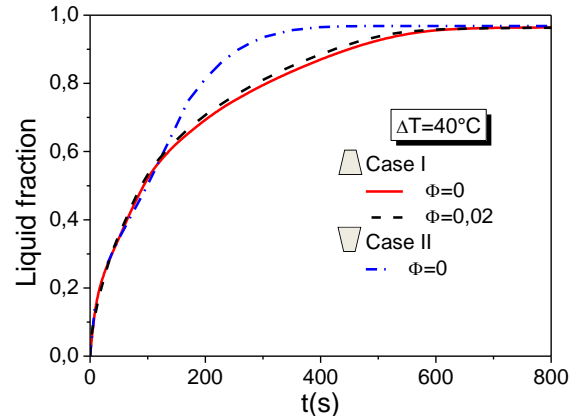


Fig.7 effect of nanoparticle on the melting rate

The instantaneous liquid fraction of pure PCM ( $\phi=0$ ) for both orientations of the cavity and NPCM ( $\phi=0.02$ ) in the cavity of case I are shown in Fig.7 at  $\Delta T=40^\circ$ . It can be seen that adding nanoparticles has insignificant effect on the melting rate of paraffin wax.

## 5 CONCLUSION

The melting process of paraffin wax inside trapezoidal heat storage units is numerically performed. A single value of nanoparticle volume concentration ( $\phi=0.02$ ) is considered since experimental works proved that there are some restrictions on the amount of nanostructures suspended in PCM such as agglomeration, precipitation and dramatic increase in viscosity. Two orientations of the cavity have been considered to study their effects on the melting rate. The numerical results have shown that adding nanoparticles does not enhance the melting. However, higher melting is attained by changing the orientation of the cavity



## REFERENCES

- [1] M.N.A. Hawlader, M.S. Uddin, M.M. Khin, Microencapsulated PCM thermal energy storage system, *Appl. Energy* 74 ,2003, 195–202.
- [2] M. Fang, G. Chen, Effects of different multiple PCMs on the performance of a latent thermal energy storage system, *Appl. Therm. Eng.* 27,2007,994–1000.
- [3] A.A. Al-Abidi, S. Mat, K. Sopian, M.Y. Sulaiman, A.Th. Mohammad, Internal and external fin heat transfer enhancement technique for latent heat thermal energy storage in triplex tube heat exchangers, *Appl. Therm. Eng.* 53, 2013, 147–156.
- [4] N. Sharifi, T.L. Bergman, M.J. Allen, A. Faghri, Melting and solidification enhancement using a combined heat pipe, foil approach, *Int. J. Heat Mass Transfer*, 78, 2014, 930–941.
- [5] J.M. Khodadadi, S.F. Hosseinzadeh, Nanoparticle-enhanced phase change materials (NePCM) with great potential for improved thermal energy storage, *Int. Commun. Heat Mass Transfer* 34 (2007) 534–543.
- [6] S.S. Sebt, M. Mastiani, S. Kashani, H. Mirzaei, A. Sohrabi, Numerical study of melting an annular enclosure filled within nano-enhanced phase change material, *Int. Therm. Sci. J.* 17 (2) (2013).
- [7] Y. Feng, H. Li, L. Li, L. Bu, T. Wang, Numerical investigation on the melting of nanoparticle-enhanced phase change materials (NEPCM) in a bottom-heated rectangular cavity using lattice Boltzmann method, *Int. J. Heat Mass Transfer* ,81, 2015, 415–425.
- [8] R.K. Sharma, P. Ganesan, J.N. Sahu, H.S.C. Metselaar, T.M.I. Mahlia, Numerical study for enhancement of solidification of phase change materials using trapezoidal cavity, *Powder Technol*, 268, 2014, 38–47.
- [9] M. Arıcı , E. Tütüncü, M. Kan, H. Karabay, Melting of nanoparticle-enhanced paraffin wax in a rectangular enclosure with partially active walls, *Int. J. Heat and Mass Transfer*, 104, 2017, 7–17.
- [10] K. Kant , A. Shukla , A. Sharma a, P.B. Biwole, Heat transfer study of phase change materials with graphene nano particle for thermal energy storage, *Solar Energy*, 146 ,2017, 453–463.
- [11] Dutil, Y., Rousse, D. R., Salah, N. B., Lassue, S. and Zalewski, L. [2011], A review on phase change materials: Mathematical modeling and simulations, *Renewable and Sustainable Energy Reviews*, Vol. 15, pp. 112-130.
- [12] Z. Haddad , Oztop. HF, Nada. EA, Mataoui. A. A review on natural convective heat transfer of nanofluids. *Renew Sustain Energy Rev* 2012;16:5363–78.
- [13] Brinkman HC (1952) The viscosity of concentrated suspensions and solution. *J Chem Phys* 20:571.
- [14] Maxwell JC (1873) A treatise on electricity and magnetism, 1<sup>st</sup> edn, vol 1. Clarendon Press, Oxford, pp 360–366.
- [15] M.M. MacDevette, T.G. Myers, Nanofluids: an innovative phase change material for cold storage systems?, *Int J. Heat Mass Transfer* 92 (2016) 550–557.
- [16] C. Gau and R. Viskanta, Melting and Solidification of a Pure Metal on a Vertical Wall, *J. Heat Transfer*, vol. 108, pp. 174-181, 1986.
- [17] A.D Brent , V.R. Voller , K.J. Reid, Enthalpy-porosity technique for modeling convection-diffusion phase change: application to the melting of a pure metal. *Numer Heat Transfe* 13, 1988, 297–318.